Food Hydrocolloids 63 (2017) 696–704

Contents lists available at ScienceDirect

Food Hydrocolloids

journal homepage: www.elsevier.com/locate/foodhyd

Whey protein gelation induced by enzymatic hydrolysis and heat treatment: Comparison of creep and recovery behavior

Maria Julia Spotti [a, b, d, *], Özgür Tarhan [a, d, e], Sam Schaffter [c], Carlos Corvalan [c], Osvaldo H. Campanella [a, c, d]

[a] Department of Food Science, Purdue University, 745 Agriculture Mall Drive, West Lafayette, 47906, IN, USA
[b] Biocolloids Laboratory, Food Technology Institute, Faculty of Chemical Engineering, National University of Litoral, 1 de Mayo 3250, 3000, Santa Fe, Argentina
[c] Department of Agricultural and Biological Engineering, Purdue University, 225 South University Street, West Lafayette, 47907-2093, IN, USA
[d] Whistler Carbohydrate Research Center, Purdue University, West Lafayette, IN, 47907, USA
[e] Department of Food Engineering, Faculty of Engineering, Usak University, Usak, 64200, Turkey

ARTICLE INFO

Article history:
Received 20 June 2016
Received in revised form
8 September 2016
Accepted 7 October 2016
Available online 8 October 2016

Keywords:
Whey proteins
Bacillus licheniformis protease
Gelation
Fractional calculus
Creep and recovery test
Circular dichroism

ABSTRACT

Whey proteins can form different types of gels depending on the method used for their preparation. The purpose of this study was to characterize and compare gels obtained by heating and enzymatic (*Bacillus Licheniformis* protease) treatments in terms of gelation kinetic, gel mechanical and microstructural properties, and conformational changes of the protein secondary structure due to protein hydrolysis/denaturation. By comparing heat- and enzyme-induced gelation it was observed that although G′ and G″ profiles looked fairly similar, heat-induced WPI gels exhibited higher G′ and G″ values than enzyme-induced gels. G′ values at 25 °C for heat-induced gels were approximately 3500 Pa, while those for enzyme-induced gels were about 850 Pa. For both gels and during temperature sweep, storage modulus G′ slightly decreased as temperature increased. Frequency sweep in both gels showed that heat-induced gels had slight frequency dependence in comparison with enzyme-induced gels that were practically independent of frequency. These results indicated that although enzyme-induced gels exhibit smaller strength they are significantly more elastic than heat-induced gels. Same behavior was found during creep and recovery test, where the macromolecular network formed by enzyme-induced gels exhibited high flexibility: 82.6% of recovery strain in the first cycle, and 79% in the second one, being more easily stretched than heat-induced WPI gels, which had 49.8% and 40.8% in the first and second cycle, respectively. The fractional derivative modeling approach applied to the creep data showed that enzyme-induced gels were more elastic than thermally generated gels. These characteristics were also observed by microcopy analysis, showing that heat-induced gels had smaller pore sizes and a denser network with more interaction zones than enzyme-induced gels. These observations may explain the larger strength and the lower elasticity of heat-induced gels which are likely due to less specific interactions among denatured whey proteins.

1. Introduction

Whey proteins, by-products of the dairy industry, represent 20% of total milk proteins and are composed of β-lactoglobulin (β-lg) (50%), α-lactalbumin (α-la) (20%), and the rest by serum albumin, immunoglobulin and minor proteins (Cayot & Lorient, 1997). They are commonly sold as whey protein concentrate (WPC) with 35–80% of proteins, and whey protein isolate (WPI) with 90% or more proteins content (Bryant & McClements, 1998).

The ability of whey proteins to form gel matrices capable of holding large amounts of water and other ingredients is extremely important for the food industry. Although gelation of whey proteins is mostly achieved by heating (Baeza, Gugliota, & Pilosof, 2003; Bertrand & Turgeon, 2007; Ikeda, 2003), it can also be achieved by high pressure treatment (Famelart, Chapron, Piot, Brule, &

* Corresponding author. Grupo de Biocoloides, Instituto de Tecnología de Alimentos, Facultad de Ingeniería Química, Universidad Nacional del Litoral, 1 de Mayo 3250, 3000, Santa Fe, Argentina.
E-mail address: juliaspotti@yahoo.com.ar (M.J. Spotti).

http://dx.doi.org/10.1016/j.foodhyd.2016.10.014
0268-005X/

Durier, 1998; Keim & Hinrichs, 2004) and a cold gelation process induced by acidification (Alting, Hamer, de Kruif, Paques, & Visschers, 2003; van den Berg, van Vliet, van der Linden, van Boekel, & van de Velde, 2007; Britten & Giroux, 2001) or by addition of salts to pre-denatured whey proteins (Barbut, 1997; Marangoni, Barbut, McGauley, Marcone, & Narine, 2000). Whey protein gelation has also been promoted by cross-linking with transglutaminase (Truong, Clare, Catignani, & Swaisgood, 2004) and by enzymatic hydrolysis (Doucet, Gauthier, & Foegeding, 2001; Ju & Kilara, 1998; Otte, Ju, Faergemand, Lomholt, Qvist, & 1996).

Hydrolysis of whey proteins with glutamyl endopeptidase obtained from *Bacillus licheniformis* (*Bacillus licheniformis* protease, BLP) specifically cleaves peptide bonds at the C-terminal side of glutamate and aspartate residues, leading to the formation of aggregates. Peptide aggregation increases with the degree of hydrolysis up to the end of the hydrolysis process. Aggregation occurs mainly due to non-covalent interactions between the peptides, and it is mostly favored (at high degree of hydrolysis) by increased hydrophobic interactions and to a lesser extent by reduced electrostatic repulsion (Creusot & Gruppen, 2007).

Heat-induced gels are produced by a denaturation-aggregation process: unfolded whey proteins interact with each other through the formation of new intra and inter-chain disulfide bonds (β-lg has two disulfide bonds and one free sulfhydryl group and α-la has four disulfide bonds) that can form a gel network.

Accurate rheological characterization of viscoelastic materials, like whey protein gels, is critical for the design of food products with desired properties, textures, and processing behaviors. Current viscoelastic models applied to characterize food products and biomaterials contain a relatively large number of parameters which frequently have vague physical meanings. In this work, it is proposed to use a simple rheological model based on fractional calculus to describe creep and recovery behavior of viscoelastic food materials. One of the advantages of this approach is that both the creep and recovery curves can be analyzed together and also the gel characterization is done using a smaller number of viscoelastic parameters than those used by current methods, thus facilitating the analysis of the data (Schaffter, Corvalan & Campanella, 2015). Fractional models have increasingly been proposed in other fields but their application to the rheological characterization of food systems is still lacking.

Although there are many studies about whey protein gelation, this work presents a comprehensive study on heat and enzyme-induced gelation of whey proteins by comparing the gelation mechanisms through rheological properties and circular dichroism, their microstructure and also their creep and recovery behavior. A novel approach to describe viscoelasticity of the gels in terms of creep and recovery behavior is also presented. The model includes only three parameters, all of which have simple physical interpretations.

2. Materials and methods

2.1. Materials

Whey protein isolate (WPI) (BiPRO) was kindly provided by Davisco Foods International Inc. (Minnesota, USA). According to manufacturer, a typical WPI batch contains 61–70% β-Lg, 23–31% α-La, 2–4% BSA, and 1–5% IGg. The percent composition was 97% w/w protein, 0.2% w/w fat, 1.9% w/w ash and 4.8% w/w moisture; all composition expressed on a dry basis. *Bacillus licheninformis* Protease (BLP) (Activity: 13.744 AU-A/G, batch no PL 100013) was kindly provided by Novozymes A/S (Bagsvaerd, Denmark). Other reagents used were of analytical grade.

2.2. Methods

2.2.1. Preparation of WPI systems

WPI solutions were prepared at a constant protein concentration of 10% (w/w) by dissolving WPI powder in Tris-HCl buffer (75 mM, pH 7.5) overnight at 4 °C. Two different types of gelation were studied: heat-induced and enzyme-induced gelation systems. In the latter case, BLP enzyme was added with a concentration of 4% (w/w, enzyme/protein). Temperature ramps used for rheology and CD measurements are described in Sections 2.2.2 and 2.2.6, respectively. Samples of both gels for microscopy analysis were prepared using the same procedure (see Section 2.2.4) and incubated in a water bath.

2.2.2. Dynamic oscillation measurements

Dynamic oscillation measurements were performed using a rheometer (AR-G2 Model from TA Instruments, Newcastle, DE, USA) with 40 mm parallel plates (1000 μm gap). The temperature of the bottom plate was controlled with a Peltier system. Samples were subjected to dynamic oscillations with a controlled strain of 1% at 1 Hz frequency. The strain used was previously determined to be within the linear viscoelastic region of the gels. For heat-induced gels, the samples (WPI 10%) were placed onto the Peltier plate that was heated from 25 °C to 90 °C at a rate of 5 °C/min, then the temperature was maintained at 90 °C for 10 min, which was enough time to allow storage modulus (G′) equilibration. After that, the samples were cooled to 25 °C at a rate of 25 °C/min and then, the temperature was maintained at 25 °C for 10 min. For enzyme-induced gels, BLP enzyme (4%, w/w) was added to the 10% (w/w) WPI solution, mixed and right after placed onto the Peltier plate for rheological measurements. The gel formation was carried out by heating the sample from 25 to 50 °C at 1 °C/min, keeping at 50 °C for 10 h and cooling to 25 °C at 1°C/min, and then maintaining at 25 °C for 60 min. In order to prevent evaporation during rheological measurements, both samples were covered on the edge with a thin layer of silicon oil. During the measurements, storage (G′) and loss (G″) moduli, and loss tangent (tan δ) were monitored as a function of time. The temperature at which the storage and loss modulus crossed over was taken as the gel point (Tung & Dynes, 1982), and the temperature (T_{gel}) at this point was evaluated. This can also be expressed as the point where the phase angle equals 45° (tan δ) = 1, which is denoted δ = 45° (Stading & Hermansson, 1990). The gel point can be defined in terms of a gel time for isothermal heating, or a gelation temperature for a ramp temperature test (Kavanagh, Clark, & Ross-Murphy, 2000). Before removing the samples from the rheometer, frequency and temperature sweep tests were conducted. Frequency sweep measurements were performed with a 1% strain and 25 °C in the frequency range from 0.01 to 100 Hz. Temperature sweep tests were carried out from 25 to 95 °C, at 1 Hz and 1% strain.

2.2.3. Creep and recovery test

Two cycles of creep and recovery were performed, in which 1 Pa of shear stress was imposed on the sample and the strain was recorded as a function of time. In the recovery phase, the shear stress was removed and the sample was allowed to recover the elastic (instantaneous and retarded) part of the deformation. The recovery strain was calculated as follows:

$$RS\ (\%) = (\text{Final strain} - \text{initial strain})/\text{initial strain} \times 100 \quad (1)$$

2.2.4. Creep and recovery model

Creep and recovery data were analyzed by using the fractional

derivative modeling approach which has been used in polymer studies and recently introduced to the characterization of food materials (David & Katayama, 2013; Jaishankar & McKinley, 2014; Schaffter, Corvalan, & Campanella, 2015).

Eq. (2) below describes creep and recovery curves in terms of the parameter α which provides an indication of the degree of elasticity of the sample; where lower values of α indicate elastic gels whereas large values indicate more viscous samples. It must be noted that, values of α range between 0 and 1, a value of 0 would be indicating a purely elastic material whereas a value of 1 means a purely viscous one. For viscoelastic materials, like the gels studied in this work, α values range between 0 and 1. Other parameters of relevance in the test are λ_1 and λ_2 which represent the inverse of the gel elastic modulus during creep and recovery, respectively. These parameters could be associated with the structure of samples and vary when the stress is applied during the creep experiment is large enough to disturb the sample structure (Schaffter et al., 2015). The fractional derivative modeling approach can be applied for small stresses (lineal viscoelastic behavior) and large stresses (non-lineal viscoelastic behavior). It should be noted that in the latter case the parameters λ_1 and λ_2, which as mentioned above are associated to the structure of the material, will depend on the applied stress in the creep test. Conversely, if the structure of the sample is not disturbed (lineal viscoelastic behavior) these parameters will not change.

$$J(t) = \frac{\varepsilon(t)}{\sigma_0} = \frac{1}{\Gamma(\alpha+1)}\left(\lambda_1\, t^{\alpha} H(t) - \lambda_2\,(t-t_m)^{\alpha} H(t-t_m)\right) \qquad (2)$$

In Eq. (2), $J(t)$ is the material compliance, with units of %/Pa, ε(t) is the instantaneous strain measured in % strain, σ(t) is the applied stress, in units of Pascal (Pa). In order to maintain a linear viscoelastic behavior in the sample a stress of 1 Pa was selected for this test, t_m is the time at which the stress is removed to initiate the recovery test, Γ is the gamma function described by Abramowitz and Stegun (1964), and $H(t)$ is the Heaviside or step function defined as:

$$H(t) = \begin{cases} 0 & if \quad t<0 \\ 1 & if \quad t>0 \end{cases} \qquad (3)$$

Although the stress used in this work was low enough to study the linear viscoelastic behavior of the sample, as explained above the model could be applied to describe the creep behavior when a high stress is applied, i.e. when the material does not behave linearly. For those cases the rheological parameters obtained would be a function of the applied stress. The rheological parameters α, λ_1 and λ_2, were determined by fitting the experimental creep-recovery data of the formed gel to Eq. (2) using the Simplex Nelder-Mead algorithm implemented in Matlab. Further details of the procedure are described by Schaffter et al. (2015).

2.2.5. Cryo-SEM microscopy

Cryo-SEM experiments were performed using a GATAN Alto 2500 Cryo Units (JEOL Ltd., Tokyo, Japan) attached to a FEI Nova Nano630 SEM (Oregon, USA). The system permits flash freezing of samples in liquid nitrogen slush followed by high vacuum sublimation of unbound water, platinum coating to minimize charge build-up and imaging at temperatures in the range of −100 to −140 °C.

Small pieces of WPI heat- and enzyme-induced gels were placed onto aluminum stubs and the stubs were secured on the specimen holder. The sample holder was rapidly plunged into the liquid nitrogen slush. The specimens were transferred under vacuum into the preparation chamber, precooled to −180 °C and allowed to equilibrate for 10 min. The sample temperature was raised to −150 °C and a fractured surface of gel was obtained by hitting the top part of the sample with a cutter. After that, the sample was sublimed inside the SEM chamber at −90 °C for 10 min for the WPI heat-induced gel, and 15 min for the enzyme-induced gel. Then, the sample was sputter-coated with platinum (120s coating) in an argon atmosphere at −120 °C. The images were recorded at 5,000, 10,000, 20,000, 40,000 and 80000X. In all cases, the imaging was performed using an accelerating voltage of 5 kV and a working distance of 5–6 mm, using an Everhart Thornley detector.

2.2.6. CD spectra measurements

Protein solutions were prepared at final concentrations of 0.1 mg/mL in 100 mM Tris-HCl buffer (75 mM, pH 7.0) for CD measurements. Data was obtained using a Jasco J-1500 Spectropolarimeter (JASCO UK Ltd., Great Dunmow, UK). The temperature ramps for heating and cooling steps were similar to that one used during the gelation tests for better comparison of results. For the heat-induced system, a temperature interval scan was taken from 25 °C to 90 °C at a 5 °C/min heating ramp, and then the protein was cooled from 90 °C to 25 °C at a 10 °C/min ramp. For the enzyme-induced denaturation system, the temperature interval scan was performed first from 25 to 50 °C with a 5 °C/min heating ramp. Then, 10 min-interval scans were taken at 50 °C for 6 h, and cooling step scans were recorded from 50 °C to 25 °C with a 5 °C/min ramp. Quartz cells with a 0.1 cm path length were used in the measurements and the scan rate used was 10 nm/min with, with a 0.2 nm band width. Recorded spectrum was an average of 2 scans from 200 to 250 nm. Results were expressed in terms of mean residual ellipticity ([θ]) in units of deg. cm/decimol (dmol), and were determined according to the following equation:

$$[\theta] = (\mathrm{MRW})/10.l.c \qquad (4)$$

where θ corresponds to the measured ellipticity angle (deg), MRW is the mean residue weight (114.63), l is the optical path length (cm), and c is the protein concentration (g/ml). All spectra were obtained by subtracting the buffer base-line from the recorded sample spectra.

2.3. Statistical analysis

All measurements were performed at least in duplicate. Mean values and their corresponding errors were calculated and are presented in graphs as coordinate pairs with their corresponding error bars. For the statistical treatment of data, StatGraphics Centurion XV software was used and analysis of variances (ANOVA) was conducted. When statistical differences were found, the Duncan's test ($\alpha = 0.05$) was carried out. Analysis and graphic presentations were performed using OriginPro 7.5 SR0 software (OriginLab Corporation, Northampton, USA).

3. Results

3.1. Gelation of heat- and enzyme-induced WPI systems

The gelation process, promoted by heating and enzyme action, was followed by monitoring changes in the storage modulus (G′) and loss modulus (G″) as a function of time and temperature; results are shown in Fig. 1A and 1B.

Fig. 1A shows heat gelation of WPI, which is similar to the heat-induced gelation of globular proteins. At the beginning of temperature ramp, both values G′ and G″ were small indicating little viscoelasticity in the samples, but they began to increase with increases in temperature. G′ increased further after reaching a temperature close to the denaturation temperature, which has been

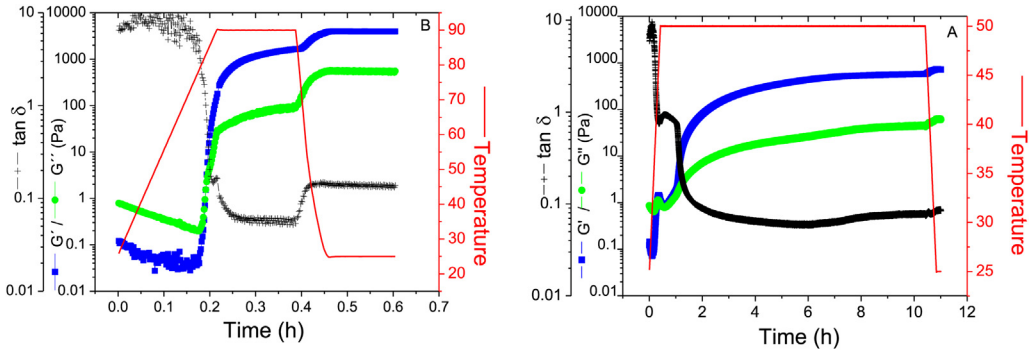

Fig. 1. Heat-induced gelation profile of 10% (w/w) WPI (A) and enzyme-induced gelation profile of 10% (w/w) WPI with 4% (w/w) BLP (B).

reported, using differential scanning calorimetry, to be around 74 °C (temperature of the peak corresponding to β-lg and a shoulder near 66 °C corresponding to α-la) according to Zhu, Damodaran, and Lucey (2010) for a 10% w/w WPI solution.

The crossover of G′ and G″ (gelation point) was not immediate, probably because protein denaturation needed some time to trigger gel formation. After 11.4 min, approximately at 82.7 °C, G′ surpassed G″, which indicated the beginning of gel network formation (Verheul, Pedersen, Roefs, & de Kruif, 1999). When a WPI solution is heated proteins undergo unfolding and lose a part or all of their native structure. If the concentration is high enough, the unfolded protein chains can interact each other and form a network due to new intra- and inter-chain disulfide bonds (β-lg has two disulfide bonds and one free sulfhydryl group and α-la has four disulfide bonds), so the gelation process occurs.

In a following stage, at a constant temperature of 90 °C for 10 min, the WPI gel network was further strengthened as more and more denatured protein molecules formed part of the network, thus increasing the elasticity of the gel. An increase in G′ value continued even further until it reached approximately 3000 Pa with decreasing temperature from 90 °C to 25 °C. The increase of G′ during cooling has been previously observed in other systems (Ould Eleya & Turgeon, 2000; Renkema & Van Vliet, 2002). This phenomenon could be attributed to a reduction in the entropy of the system, which consolidated the attractive forces (hydrogen bonding, van der Waals forces) between protein particles in the gel (Chronakis & Kasapis, 1993; Manoj, Kasapis, & Hember, 1997). The loss modulus G″ showed a similar trend as a function of time, but its values remained much lower than G′, which clearly indicated that an elastic gel was formed.

The enzyme-induced WPI gel showed a similar profile (Fig. 1B). G′ and G″ started to increase with the increase of temperature, but G′ increased faster than G″, and tan δ decreased significantly. The gel point was recorded as the crossing over point of G′ and G″. G′ increased until 650 Pa in a few hours and this value was almost constant for 6 h approximately. When the temperature decreased from 50 to 25 °C, an increase of G′ values was observed (850 Pa) because of the consolidation of noncovalent interactions, as it was previously observed and hypothesized for heat-induced gels.

Gels obtained by enzymatic hydrolysis are produced at 40–50 °C (Doucet et al., 2001) because the BLP enzyme is more active at that temperature and a pH range between pH 6.5 and pH 8.5 (BLP has an optimum activity temperature of 50 °C). Enzymatic hydrolysis of proteins causes a decrease in their molecular weight, an increase in the number of ionizable groups, and an enhanced exposure of hydrophobic groups (Panyam & Kilara, 1996). Aggregation, then, proceeds with further association among protein particles by non-covalent interactions, thus creating a three-dimensional network.

Doucet et al. (2001) showed that aggregation and gelation occurred after an extensive hydrolysis of WPI with Alcalase 2.4L (an enzyme from *Bacillus licheniformis*). They reported that hydrophobic interactions among peptides, with a molecular mass less than 2 kDa were involved in the formation of aggregates, which further were associated to form a gel. Otte et al. (1996) showed that the partial hydrolysis of WPI with a serine protease from *Bacillus licheniformis* (BLP) also led to aggregation and gelation. According to Otte et al. (1997) β-lg, is the most abundant protein in bovine whey. So it is considered the main protein responsible for the gelation in WPI when BLP is used for hydrolysis. In their study, they found that the hydrolysis of a purified preparation of β-lg formed a gel at a concentration of 7% (w/v). Graveland-Bikker, Ipsen, Otte, and de Kruif (2004) studied the hydrolysis of α-la, the second major protein in bovine whey, with BLP and found that this system also led to the formation of aggregates and under certain conditions nanotubutes of α-la.

By comparing heat- and enzyme-induced gelation it can be observed that although G′ and G″ profiles of Fig. 1A and B look similar, heat-induced WPI gels (Fig. 1A) showed higher G′ and G″ values than enzyme-induced gels (Fig. 1B). G′ values at 25 °C (average of final values) for heat-induced gels were approximately 3500 Pa, while for enzyme-induced gels G′ values were approximately 850 Pa. Based on Fig. 1, temperature at the crossing point of G′ and G″ (T_{gel}) was 82.7 °C for heat-induced gels and 42.7 °C for BLP gels. Tan δ, which is an indicator of the relative viscoelasticity of the gels, had a value of 0.14 for heat-induced gels, and 0.08 for enzyme-induced gels. According to Avanza, Puppo, and Añón (2005), a system with a tan $\delta > 0.6$ is associated with a weak gel behavior, whereas tan $\delta < 0.15$ indicates elastic gel behavior. These values show that both heat and enzyme-induced systems are true gels but the BLP induced gels are significantly more elastic than heat-induced gels despite of the fact that the value of the storage modulus G′ was significantly larger for heat-induced gels. It is important to note that the sole value of the storage modulus is not indicative of the elasticity of a gel. Instead it provides the strength of the gel. From the results it becomes apparent that heat-induced gels have a larger strength than enzyme-induced gels probably as a consequence of the aggregation of larger molecules (denatured proteins). Conversely for BLP enzyme gels aggregation of smaller peptides are responsible of gelation. Thus, enzyme-induced gels have less strength but they are significantly more elastic as indicated by the lower values of tan δ.

3.2. Frequency sweep measurements

Mechanical spectra of both types of gels are given in Fig. 2. Dependence of elastic modulus with frequency gives information on the gel structure (Stading & Hermansson, 1990). According to

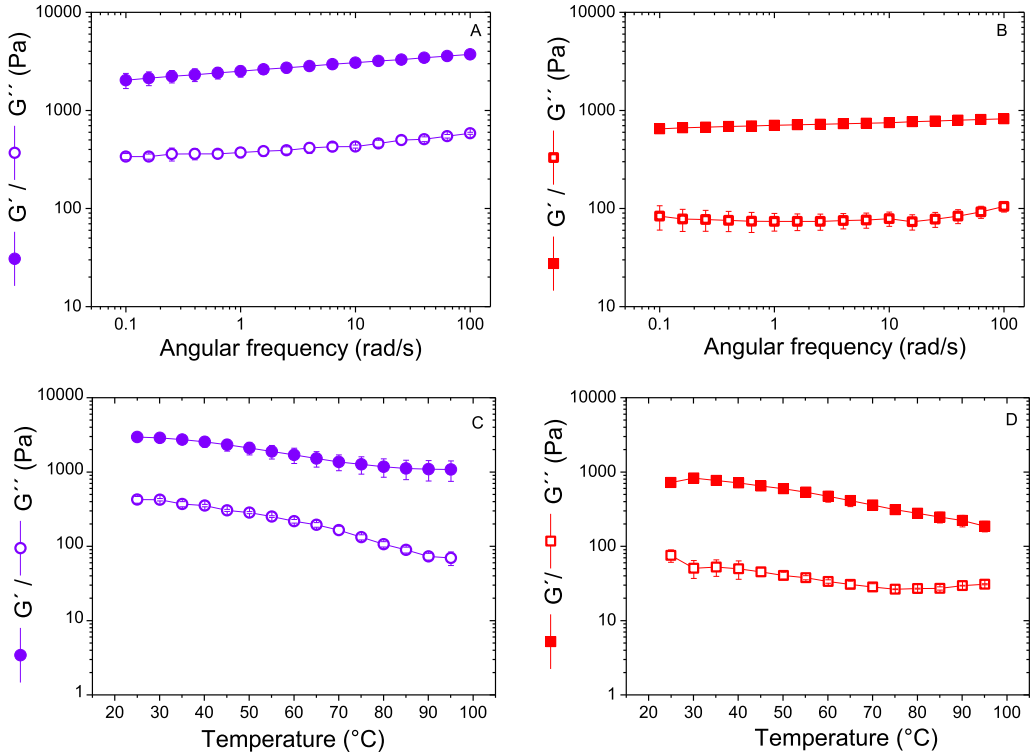

Fig. 2. Frequency sweep curves of heat-induced WPI (10%, w/w) gel (●) (A) and BLP (4%, w/w)-induced WPI (10%, w/w) gel (■) (B); and temperature sweep curves from 25 to 95 °C of heat-induced WPI (10 %, w/w) gel (●) (C) and BLP (4% w/w)-induced WPI (10%, w/w) gel (■) (D).

Stading and Hermansson (1990) the dependence of G′ and G″ with frequency shows the type of gels formed: strong gels show very little frequency dependence and do not exhibit G′ and G″ crossover, they resemble covalent or chemical gels. However, physical gels show frequency dependence, in contrast to covalent/chemical gels, without G′ and G″ crossover. The gels that show both frequency dependence and G′ and G″ crossover are considered to be formed by entanglement of molecules and for that reason they are called "entanglement network systems". As shown in Fig. 2, neither heat-induced nor enzyme-induced gels showed G'and G″ cross over in their mechanical spectra.

Heat-induced gels showed a slight frequency dependence (Fig. 2A) in comparison with enzyme-induced gels that showed practically no dependence (Fig. 2B). These results show that although enzyme-induced gels have smaller strength they are significantly more elastic than heat-induced gels. This could indicate that enzyme induced gels are formed by a fine stranded network structure consisting of ordered arrangements of molecules that promote a larger elasticity.

3.3. Temperature sweep measurements

In order to determine the type of interactions involved in the heat-induced and enzyme-induced gels, temperature sweep tests were conducted (Fig. 2C and D). The rubber elastic theory states that G′ should increase with temperature (Ferry, 1980). In this study, none of the formed gels followed that relationship. For both gels, the storage modules G′ slightly decreased as temperature increased. Similar results were found by Doucet et al. (2001) while working with heat-induced and enzyme-induced WPI gels.

Although hydrogen bonds are not usually the major driving force determining the conformation and aggregation of globular proteins, they do play an important role in stabilizing the structures once formed (Kinsella & Whitehead, 1989). When the temperature increase, hydrogen bonds become weaker because the entropy increases, so G′ decreases as well. Moreover, hydrophobic interactions increase as the temperature is raised (Baldwin, 1986) up to 60–70 °C, a further increase in temperature produces attenuation of these interactions (Bryant & McClements, 1998). This is in agreement with the results illustrated in Fig. 2C and D where it is noted that a more significant decrease of the storage modulus is starting at temperatures higher than 60 °C. Also note in Fig. 2 that the decrease in G′ for heat-induced WPI gel (G′ at the end of heating is 40% of the initial value) is less than that observed in G′ for the enzyme-induced gel (30% of the initial value). This small difference could be attributed to the more specific interactions between small peptides for the formation of aggregates that contribute to form more elastic gels.

3.4. Creep and recovery behaviors of heat- and enzyme-induced WPI gels

Creep-recovery curves of heat and enzyme-induced gels are presented in Fig. 3A. Creep curves showed similar viscoelastic performance but they were different in maximum strain.

According to Fig. 3A, the macromolecular network formed in enzyme-induced gel tends to be more flexible so that the gel is more easily stretched than heat-induced WPI gel (Qiu-liang, Shen, & Si-ming, 2009). The network in heat-induced WPI gels is formed by disulfide bonds and they are responsible for greater stiffness as discussed previously in terms of the larger G′ values of these gels. In contradiction, the main forces responsible for the formation of the matrix in enzyme-induced gels are due to more specific interaction of smaller and more mobile peptides. Both gels display typical creep curves of viscoelastic materials. In addition, an irrecoverable strain is observed at the end of the recovery test. According to

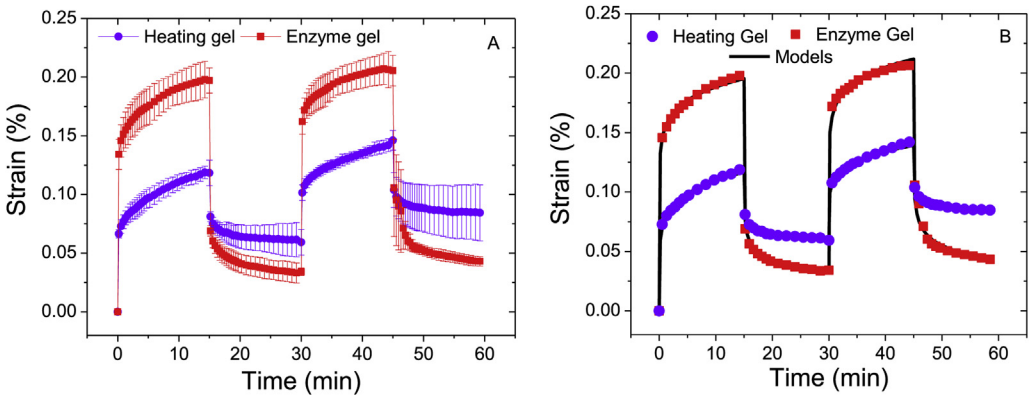

Fig. 3. Creep and recovery (two cycles) curves for heat-induced WPI (10%, w/w) gel (●) and BLP (4%, w/w)-induced WPI (10%, w/w) gel (■) (A); fit model for both gel systems: the heat-induced data is depicted as circles with a fit model in red and the enzyme induced data is depicted as triangles with a fit model in black (B). The $t'_m s$ for the experiments were both 15 min.

Lefebvre, Renard, and Sanchez-Gimeno (1998), the existence of an irrecoverable strain does not necessarily imply the existence of material with having a considerable viscous component that dissipates the deformation energy and it is not recovered when the stress is taken off.

The recovery strain in heat-induced WPI gels was 49.8% in the first cycle, and 40.8% in the second one. For enzyme-induced gels, the recovery strain was 82.6%, and 79.0% indicating as suggested by the other viscoelastic tests that enzyme-induced gels are significantly more elastic than heat-induced gels but having a small strength.

3.5. Creep and recovery modeling

The fractional derivative based creep parameters for WPI heat and enzyme-induced gels are shown in Table 1, and the fitting curves are shown in Fig. 3B. As illustrated, the enzyme-induced gel (WPI-E) has lower α values than those of the heat-induced gel (WPI-H) for the 1st and 2nd creep. The parameter α varies between 0 and 1. The closer the parameter is to 1 the more viscous is the material, being $\alpha = 1$ for a perfectly viscous material and $\alpha = 0$ for a perfectly elastic material. From this standpoint, the enzyme-induced gel is more elastic than the heat-induced gel. These results are in full agreement with the results presented in the previous section.

Materials which are permanently deformed during the creep test because the applied stress is affecting the material structure may have a larger resistance to recovery and thus a lower λ_2 value than that of λ_1. Physically it means that as a consequence of the breaking of the material structure by the high shear applied during the creep test the material loose ability to recover the strain. The value of λ_2 can take on values between 0 (infinite resistance which leads to no recovery) and λ_1 i.e. when the recovery path is the same as the creep path and the material deforms and recovers linearly.

Table 1
Fitting parameters for model of heat-induced sample. The fit of this data is shown by the red curve in Fig. 6.

Creep and recovery	Derivative order (α)	Creep constant ($\lambda_1\sigma_o$)	Recovery constant ($\lambda_2\sigma_o$)	$\lambda_1-\lambda_2$
1st creep H-WPI	0.154	0.072	0.042	0.03
2nd creep H-WPI	0.158	0.048	0.040	0.008
1st creep E-WPI	0.088	0.147	0.132	0.015
2nd creep E-WPI	0.098	0.130	0.132	−0.002

Parameters obtained by modeling the averages of duplicate tests for each system.

Thus, the evaluation of (λ_1-λ_2) is useful when comparing the way that materials recover. A material with a larger difference between these two parameters has a greater degree of permanent deformation, probably a significant change in its structure and different rheological behavior during creep and recovery.

According to Table 1, during the first creep the difference between λ_1 and λ_2 for heat-induced gels is higher than in the second creep (0.03, and 0.008, respectively). Same behavior is observed for enzyme-induced gels, but in this later case the differences are even lower, being 0.015 in the first creep and 0.02 in the second. As previously mentioned, the difference between λ_1 and λ_2 can be compared to assess the "recoverability" of a material after creep. In general smaller differences between these parameters are indicating materials with more ability to recover, and a more elastic character as observed in the enzyme-induced gels.

3.6. Gel microstructure

SEM images of both gels at different magnifications are shown in Fig. 4. The microstructure of heat-induced gels can be observed in the first row of the series of pictures whereas the one from the enzyme-induced gels are illustrated in the second row. It can be clearly seen that, the heat-induced gel has a smaller pore size, and the network is denser than that of enzyme-induced gels, and with more interaction points. That explains the larger strength and the lower elasticity of the heat-induced gels likely resulting of less specific interactions among denatured whey proteins. Heat-induced WPI gels have a fine-stranded gel structure, and enzyme-induced WPI gels showed thicker filaments forming the network with a more open structure. The open structure and thicker strands may indicate lesser interaction points in these gels but stronger bonds leading to higher elasticity.

These results are in accordance with the rheology measurements, since the smaller the pore size the higher the gel strength, and higher G′ values were obtained for heat-induced WPI gels at the end of gelation process in comparison to enzyme-induced gels.

The macroscopic visual appearances of the gels are shown in Fig. 4. The heat-induced gels were transparent, while enzyme-induced gels were more opaque, glossy and white. These macroscopic appearances can be explained in terms of microstructure since the gels formed depend on the nature of the protein aggregates. A solution of filamentous aggregates appears transparent because the width of the filaments is so small that they do not scatter light strongly. On the other hand, a solution of particulate aggregates appears optically opaque because the formed strands

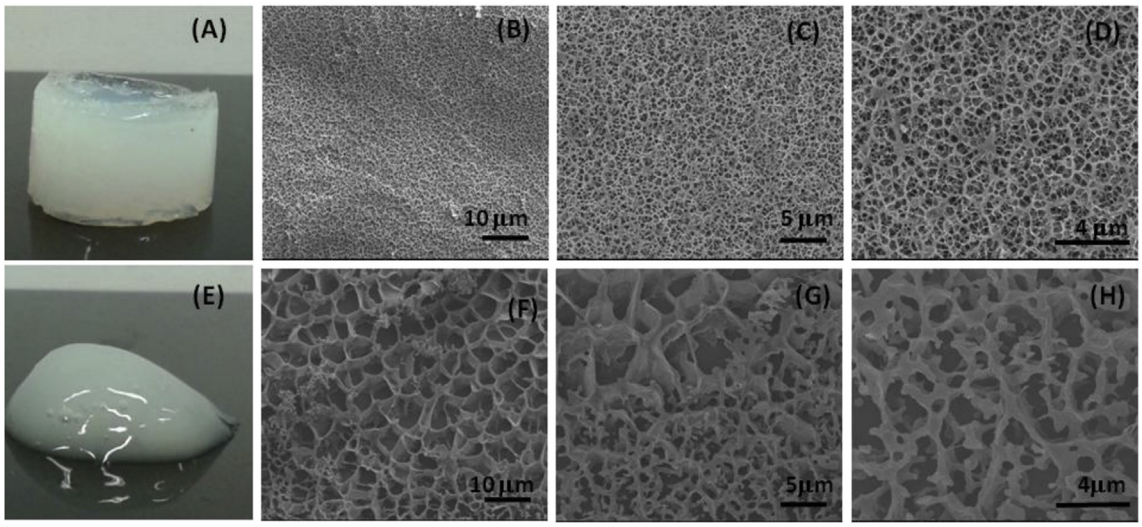

Fig. 4. Image of WPI 10% w/w heat-induced gel (A) and its cross section images by cryoscanning electron microscopy (cryo-SEM) at 5000 (A), 10,000 (B), and 20,000 X; and image of WPI 10% w/w-4% w/w BLP gel and its cryo-SEM images at 5,000 (F), 10,000 (G), and 20,000 X (H).

are thicker and have more influence on the scattering the light (Bryant & McClements, 1998).

3.7. CD spectra measurements

Globular proteins have a characteristic secondary structure in their native state, i.e. they contain specific amounts of α-helix, β-sheet, and random coil conformations. When a globular protein solution is heated or subjected to enzymatic degradation unfolds and loses a part of its secondary structure. Due to protein denaturation and further aggregation, the development of a newly ordered structure (such as β-sheet) often occurs. CD spectroscopy is a technique commonly used to assess the relative proportions of the different secondary structures present in both native and denatured forms of a protein.

When circularly polarized light passes through an optically absorbing sample, the speeds between right and left polarization differ as well as their wavelengths and the extent to which they are absorbed (Chandrapala, Zisu, Palmer, Kentish, & Ashokkumar, 2011). One of the two polarized light beams is absorbed more than the other, and this difference in absorption, which is wavelength dependent, is measured yielding the CD spectrum (Chandrapala et al., 2011). For example, α-helical proteins have negative bands at 222 nm and 208 nm and a positive band at 193 nm. Proteins with well-defined antiparallel β-pleated sheets (β-helices) have negative bands at 218 nm and positive bands at 195 nm, while disordered proteins have very low ellipticity above 210 nm and negative bands near 195 nm (Greenfield, 2006). The secondary structure of β-lg comprises nine β-strands, a short α-helix segment and three helicoidal turns (Chandrapala et al., 2011).

In Fig. 5 the ellipticity of WPI during heating from 25 to 90 °C and during cooling from 90 to 25 °C is illustrated. During heating, there is a tendency to decrease the ellipticity near 208 nm, while the values near 222 and 218 nm are almost the same. This decrease is more accentuated when the temperature exceeds 70 °C, being in accordance with the denaturation temperature of WPI, which as discussed above has been estimated as approximately 74 °C (Zhu et al., 2010). This increase in the signal could be related to an increase in α-helix content and a decrease of β-turns. However, Kavanagh et al. (2000) found that CD spectra recorded over a range of temperatures 25–85 °C shows that about 50% of the secondary structure of β-lg, is in a β-sheet form, for both the native protein and its aggregates. Increasing the temperature produced only a slight increase in β-sheet content. Fig. 5B shows that during cooling there is a small increase in the ellipticity near a wavelength of 210 nm, but no differences were found analyzing the punctual data at wavelengths 208, 222 and 218 nm.

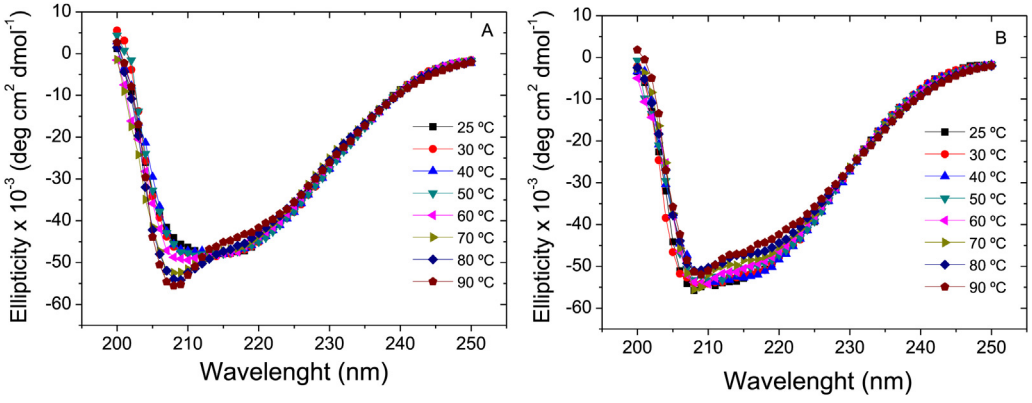

Fig. 5. CD data of heat-induced WPI (10%, w/w) gel during heating from 25 °C to 90 °C (A) and cooling from 95 to 25 °C (B).

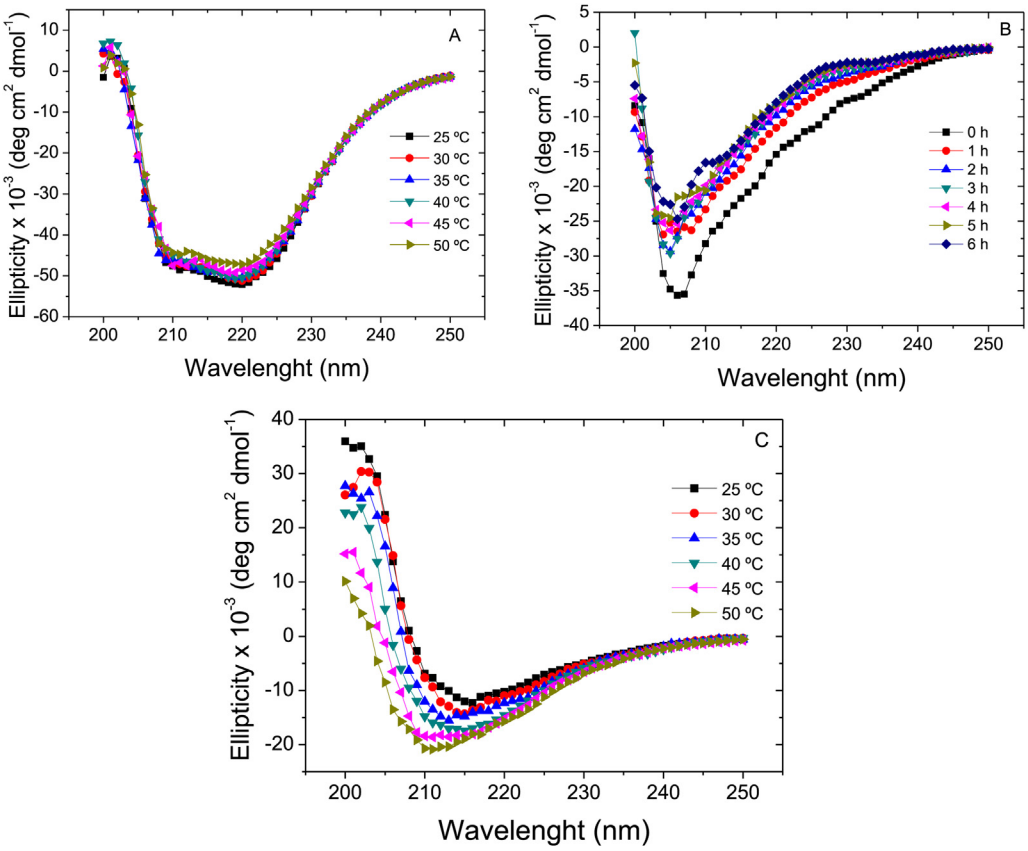

Fig. 6. CD data of BLP (4%, w/w)-induced WPI (10%, w/w) gel at different temperatures during heating from 25 °C to 50 °C (A), maintenance at 50 °C for 6 h (B) and cooling from 50 °C to 25 °C (C).

The secondary structure of a protein depends not only on the local sequence of amino acids but also on the interactions between them. It is possible that these interactions are altered by heating. However, the CD signals reveals that the secondary structure conformation of WPI remained unaltered. Probably, the tertiary structure could be more affected by heating. Unfortunately, no tertiary structure changes were studied. To study tertiary structure changes CD signals arising from aromatic amino acids must be followed by measurement in the region 260–320 nm, which could not be achieved with the CD instrument used in this research.

In enzyme-induced gels, there is a shift to higher values of ellipticity when the temperature increased from 25 to 50 °C (Fig. 6A). The presence of a peak minimum at 218 nm confirms that WPI exhibits predominantly a β-strand behavior (Kelly, Jess, & Price, 2005).

When the temperature is maintained at 50 °C for 6 h (Fig. 6B), there is a considerable increase in the ellipticity values near 208 nm, mostly in the first hour. This can be related to the results of the oscillatory rheological tests, which showed that G′ increases quickly in the first hour of the test (Fig. 1B). During cooling from 50 °C to 25 °C (Fig. 6C) there is another shift to higher values. In spite of this little changes in CD signals, the secondary structure of the peptides of WPI appear to be retained. It is likely that the low concentrations of those structure cannot be detected by the CD measurements making the determination of those changes undistinguishable.

4. Conclusions

Heat- and enzyme-induced gels of whey protein isolate were obtained. Circular dichroism analysis revealed that changes in the secondary structure of the proteins were not very significant. The different methods for obtaining both types of gels had a significant impact in the gels physical and mechanical properties. Heat-induced whey protein gels were stiffer but less elastic than enzyme-induced gels, as seen by rheological results such as mechanical spectra and creep and recovery data. The parameters obtained with the creep and recovery model by a fractional derivative modeling approach also showed these different types of behavior. The microstructure of both gels revealed why the gels had these differences. A dense and regular structure was observed for heat-induced gels, meanwhile enzymatic gels showed an open and looser structure.

Acknowledgements

The authors would like to thank Chia Ping Huang from Life Science Microscopy Facility, Dr. Aaron Taylor from Bioscience Imaging Facility and Dr. Patricia Bishop from Chemistry Department in Purdue University for their technical assistance in cryo-SEM, confocal microscopy and CD analyses, respectively. The author Dr. Ozgur Tarhan was financially supported by The Scientific and Technological Research Council of Turkey (TUBITAK) for post-doctoral research in USA. Dr. Julia Spotti was financially supported by The National Scientific and Technical Research Council (CONICET).

References

Abramowitz, M., & Stegun, I. A. (1964). *Handbook of mathematical functions with*

formulas, graphs, and mathematical tables (1st ed.). Washington: United States Department of Commerce, National Bureau of Standards (NBS).
Alting, A. C., Hamer, R. J., de Kruif, C. G., Paques, M., & Visschers, R. W. (2003). Number of thiol groups rather than the size of the aggregates determines the hardness of cold set whey protein gels. *Food Hydrocolloids, 17*, 469–479.
Avanza, M. V., Puppo, M. C., & Añón, M. C. (2005). Rheological characterization of amaranth protein gels. *Food Hydrocolloids, 19*, 889–898.
Baeza, R., Gugliota, L., & Pilosof, A. (2003). Gelation of β-lactoglobulin in the presence of propylene glycol alginate: Kinetics and gel properties. *Colloids and Surfaces B: Biointerfaces, 31*(1–4), 81–93.
Baldwin, R. L. (1986). Temperature dependence of the hydrophobic interaction in protein folding. *Proceedings of the National Academy of Sciences USA, 83*, 8069–8072.
Barbut, S. (1997). Relationship between optical and textural properties of cold-set whey protein gels. *Lebensmittel-Wissenschaft & Technologie, 30*, 590–593.
van den Berg, L., van Vliet, T., van der Linden, E., van Boekel, M. A., & van de Velde, F. (2007). Breakdown properties and sensory perception of whey proteins/polysaccharide mixed gels as a function of microstructure. *Food Hydrocolloids, 21*, 961–976.
Bertrand, M.-E., & Turgeon, S. L. (2007). Improved gelling properties of whey protein isolate by addition of xanthan gum. *Food Hydrocolloids, 21*, 159–166.
Britten, M., & Giroux, H. J. (2001). Acid-induced gelation of whey protein polymers: Effects of pH and calcium concentration during polymerization. *Food Hydrocolloids, 15*, 609–617.
Bryant, C. M., & McClements, D. J. (1998). Molecular basis of protein functionality with special consideration of cold-set gels derived from heat-denatured whey. *Trends in Food Science & Technology, 9*, 143–151.
Cayot, P., & Lorient, D. (1997). Structure-function relationships of whey proteins. In S. Damodaran, & A. Paraf (Eds.), *Food proteins and their applications*. New York: Marcel Dekker. pp. 225e 256.
Chandrapala, J., Zisu, B., Palmer, M., Kentish, S., & Ashokkumar, M. (2011). Effects of ultrasound on the thermal and structural characteristics of proteins in reconstituted whey protein concentrate. *Ultrasonics Sonochemistry, 18*, 951–957.
Chronakis, I. S., & Kasapis, S. (1993). Structural properties of single and mixed milk/soya protein systems. *Food Hydrocolloids, 7*, 459–478.
Creusot, N., & Gruppen, H. (2007). Enzyme-induced aggregation and gelation of proteins. *Biotechnology Advances, 25*, 597–601.
David, S. A., & Katayama, A. H. (2013). Fractional order for food gums: Modeling and simulation. *Applied Mathematics, 4*, 305–309.
Doucet, D., Gauthier, S. F., & Foegeding, E. A. (2001). Rheological characterization of a gel formed during extensive enzymatic hydrolysis. *Journal of Food Science, 66*, 711–715.
Famelart, M.-H., Chapron, L., Piot, M., Brule, G., & Durier, C. (1998). High pressure-induced gel formation of milk and whey concentrates. *Journal of Food Engineering, 36*, 149–164.
Ferry, J. D. (1980). *Viscoelastic properties of polymers* (3rd ed.). New York: John Wiley (Chapter: Dependence of Viscoelastic Behavior on Temperature and Pressure).
Graveland-Bikker, J. F., Ipsen, R., Otte, J., & de Kruif, C. G. (2004). Influence of calcium on the self-assembly of partially hydrolyzed alpha-lactalbumin. *Langmuir, 20*(16), 6841–6846.
Greenfield, N. J. (2006). Using circular dichroism spectra to estimate protein secondary structure. *Nature Protocols, 1*(6), 2527–2535.
Ikeda, S. (2003). Heat-induced gelation of whey proteins observed by rheology, atomic force microscopy, and Raman scattering spectroscopy. *Food Hydrocolloids, 17*, 399–406.
Jaishankar, A., & McKinley, G. H. (2014). A fractional K-BKZ constitutive formulation for describing the nonlinear rheology of multiscale complex fluids. *Journal of Rheology, 58*, 1751–1788.
Ju, Z. Y., & Kilara, A. (1998). Gelation of hydrolysates of a whey protein isolate induced by heat, protease, salts and acid. *International Dairy Journal, 8*, 303–309.
Kavanagh, G. M., Clark, A. H., & Ross-Murphy, S. B. (2000). Heat-induced gelation of globular proteins: Part 3. Molecular studies on low pH β-lactoglobulin gels. *International Journal of Biological Macromolecules, 28*, 41–50.
Keim, S., & Hinrichs, J. (2004). Influence of stabilizing bonds on the texture properties of high-pressure-induced whey protein gels. *International Dairy Journal, 14*, 355–363.
Kelly, S. M., Jess, T. J., & Price, N. C. (2005). How to study proteins by circular dichroism. *Biochimica et Biophysica Acta, 1751*, 119–139.
Kinsella, J. E., & Whitehead, D. M. (1989). Proteins in whey: Chemical, physical, and functional properties. *Advances in Food and Nutrition Research, 33*, 343–438.
Lefebvre, J., Renard, D., & Sanchez-Gimeno, A. C. (1998). Structure and rheology of heat-set gels of globular proteins I. Bovine serum albumin gels in isoelectric conditions. *Rheologica Acta, 37*, 345–357.
Manoj, P., Kasapis, S., & Hember, M. W. N. (1997). Sequence-dependent kinetic trapping of biphasic structures in maltodextrin–whey protein gels. *Carbohydrate Polymers, 32*, 141–153.
Marangoni, A. G., Barbut, S., McGauley, S. E., Marcone, M., & Narine, S. S. (2000). On the structure of particulate gels: The case of salt-induced cold gelation of heat-denatured whey protein isolate. *Food Hydrocolloids, 14*, 61–74.
Otte, J., Ju, Z. Y., Faergemand, M., Lomholt, S. B., & Qvist, K. B. (1996). Protease-induced aggregation and gelation of whey proteins. *Journal of Food Science, 61*, 911–915.
Otte, J., Lomholt, S. B., Ipsen, R., Stapelfeldt, H., Bukrinsky, J. T., & Qvist, K. B. (1997). Aggregate formation during hydrolysis of à-lactoglobulin with a Glu and Asp specific protease from *Bacillus licheniformis*. *Journal of Agricultural and Food Chemistry, 45*, 4889–4896.
Ould Eleya, M. M., & Turgeon, S. L. (2000). Rheology of k-carrageenan and β-lactoglobulin mixed gels. *Food Hydrocolloids, 14*, 29e40.
Panyam, D., & Kilara, A. (1996). Enhancing the functionality of food proteins by enzymatic modification. *Trends in Food Science & Technology, 71*, 120–125.
Qiu-liang, Z., Shen, Y., & Si-ming, Z. (2009). Study on creep model of rice gel. In *Computational intelligence and software engineering, 2009. CiSE 2009. International conference on (pp. 1e5)*.
Renkema, J. M. S., & Van Vliet, T. (2002). Heat-induced gel formation by soy proteins at neutral pH. *Journal of Agricultural and Food Chemistry, 50*, 1569–1573.
Schaffter S., Corvalan C.M., and Campanella O.H. 2015. A creep and recovery model based on fractional calculus for the characterization and design of viscoelastic food materials (internal communication).
Stading, M., & Hermansson, A. M. (1990). Viscoelastic behaviour of β-lactoglobulin structures. *Food Hydrocolloids, 4*(2), 121–135.
Truong, V. D., Clare, D. A., Catignani, G. L., & Swaisgood, H. E. (2004). Cross-linking and rheological changes of whey proteins treated with microbial transglutaminase. *Journal of Agricultural and Food Chemistry, 52*, 1170–1176.
Tung, C. Y. M., & Dynes, P. J. (1982). Relationship between viscoelastic properties and gelation in thermosetting system. *Journal of Applied Polymer Science, 27*, 569.
Verheul, M., Pedersen, J. S., Roefs, S. P. F. M., & de Kruif, K. G. (1999). Association behavior of native β-lactoglobulin. *Biopolymers, 49*, 11–20.
Zhu, D., Damodaran, S., & Lucey, J. A. (2010). Physicochemical and emulsifying properties of whey protein isolate (WPI)-dextran conjugates produced in aqueous solution. *Journal of Agricultural and Food Chemistry, 58*, 2988–2994.